chemosensors

MDPI

Review

Tesla Valve Microfluidics: The Rise of Forgotten Technology

Agnes Purwidyantri [1] and Briliant Adhi Prabowo [2,*]

[1] School of Chemistry and Chemical Engineering, Queen's University Belfast, David Keir Building, 14 Stranmillis Road, Belfast BT9 5AG, UK
[2] School of Mathematics and Physics, Queen's University Belfast, Main Physics Building, University Road, Belfast BT7 1NN, UK
* Correspondence: b.prabowo@qub.ac.uk

Abstract: The Tesla valve (TV), a valvular conduit invented by Nicola Tesla over a century ago, has recently acquired significant attention and application in various fields because of the growing interest in microfluidics and nanofluidics. The unique architecture of TV characterized by an asymmetrical design and an arc-shaped channel has long been an intriguing yet underrated design for building a passive component in a microfluidic system. While previously regarded as a technology without significant use, TV structures have been implemented in thermal manipulation fluidics, micromixers and micropumps, benefitting the advancement of urgently demanding technology in various areas, such as in biomedical diagnostics through wearable electronics and medical instruments, lab on a chip, chemosensors and in application toward sustainable technology manifested in fuel cell devices. This article presents the first comprehensive review of TV structures in the literature, which has seen significant growth in the last two years. The review discusses typical TV structures, including single-stage TV (STV), multistage TV (MSTV), and TV derivatives (TVD), along with their characteristics and potential applications. The designs of these structures vary based on their intended applications, but all are constructed based on the fundamental principle of the TV structure. Finally, future trends and potential applications of TV structures are summarized and discussed. This topical review provides a valuable reference for students, early-career scientists, and practitioners in fluidic devices, particularly those interested in using TV structures as passive components.

Keywords: Tesla; valve; microfluidics; valvular conduit; rectifier fluid

Citation: Purwidyantri, A.; Prabowo, B.A. Tesla Valve Microfluidics: The Rise of Forgotten Technology. *Chemosensors* **2023**, *11*, 256. https://doi.org/10.3390/chemosensors11040256

Academic Editor: Jin-Ming Lin

Received: 6 March 2023
Revised: 12 April 2023
Accepted: 18 April 2023
Published: 20 April 2023

1. Introduction

The Tesla valve (TV) is a fascinating invention that has a rich history. It was first patented in 1920 by Nikola Tesla, who was a renowned scientist and inventor in electromagnetic physics [1]. Tesla was inspired by his previous invention, the electronic rectifier [2], to design a device that could be used as a unidirectional conduit for fluids [3]. The valve's structure comprises a series of interconnected channels and obstructions that allow fluid to flow in one direction but restrict it from flowing in the opposite direction. TV has been extensively studied for their potential use in various applications, including fluidic control, energy devices, and biomedical engineering. The TV is unique because it relies solely on an asymmetrical channel design without the use of moving mechanical parts to rectify a fluid flow (Scheme 1). Despite their innovative design, TVs were initially overlooked as a technology without significant use and were considered a forgotten technology for many years [3,4]. However, in recent years, researchers have explored the potential of TVs in various applications, particularly in microfluidics. TVs have been useful in situations where low flow rates are required or in microfluidic devices where moving parts can cause complications or reduce the device's overall efficiency.

Interestingly, the TV phenomenon has also been found in nature. The physical mechanism of the TV has been noted in the spiral intestine of sharks, skates, and rays where its natural design crucially reinforces nutrient absorption because of the higher friction

between the dissolved meals and the spiral intestine walls [5,6]. This natural TV-like geometry in these species significantly provides greater surface area for the process of nutrient absorption and digestion.

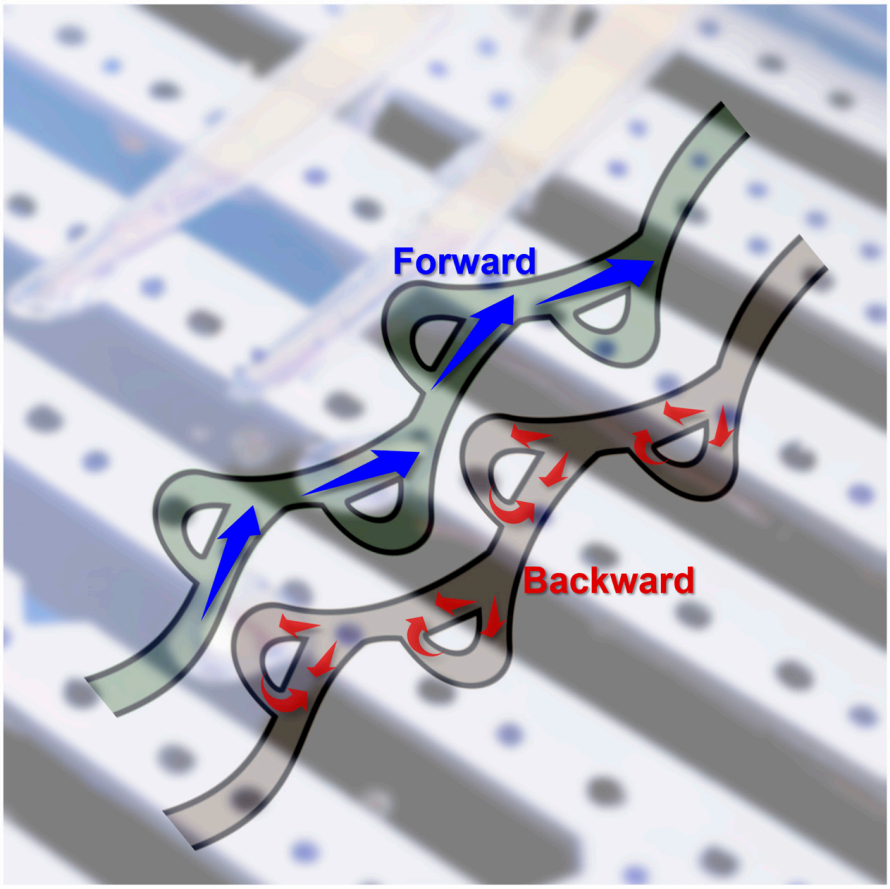

Scheme 1. The main principle of the TV is showing one-directional flow using asymmetrical structures of the channel.

Besides the shark's spiral intestine, the TV structure has also been resemblant to the turtle's lung anatomy [7,8]. The lung is composed of four large lateral chambers and several smaller medical chambers. There is a broad intrapulmonary bronchus that traverses the lung in a zigzag pattern, supporting the total respiratory physiology. The natural occurrence of TV geometry has inspired various microfluidic configurations, aiming to harness the efficiency of a gas or fluidic transport and manipulation for several applications.

Using TV microchannels has been essential in a variety of applications, including as a valve, flow resistance, and micromixer because of their unique asymmetrical flow direction [9–11]. One of the key advantages of using a TV channel as a passive component in a microfluidic system is its integration with a channel in a plane dimension. This means that only a single-layer fabrication step is required in soft lithography fabrication, resulting in a simpler and more cost-effective manufacturing process. Another significant advantage of the TV channel is its reliability, as it does not require any moving parts, such as membranes, cantilevers, or spherical balls, which can be prone to mechanical failure [10,12]. This robustness and durability make the TV channel an attractive option for microfluidic devices, particularly those intended for harsh or demanding environments. Recent advancements in artificial intelligence and machine learning have opened new opportunities for the optimization and customization of TV microchannels for specific applications. By using algorithms and simulations, researchers can design and optimize TV channels with tailored properties, such as flow resistance and valve function, to meet

specific requirements and enhance the overall efficiency of microfluidic devices. This integration of artificial intelligence (AI) and TV technology is expected to lead to further breakthroughs in microfluidics, enabling the development of highly efficient and reliable devices for a wide range of applications.

Besides its advantages over traditional valve designs, the Tesla valve has been found to offer a more comprehensive range of flow rates, with a constant diodicity in higher fluid flow rates [13], when compared to other passive valve designs, such as wing arrays. This unique feature of the Tesla valve makes it universally applicable for a wide range of applications, including in fuel cell devices for the gas flow of hydrogen decompression [14,15]. The diodicity performance of the TV channel can be further optimized by employing different periodicity and curvature designs of the structures [9,16]. Researchers have explored various design strategies to enhance the performance of the TV channel, such as by altering the spiral angle or introducing modifications to the channel geometry. These modifications can lead to significant improvements in the diodicity performance of the channel, increasing its overall efficiency and effectiveness. Figure 1 displays the characteristics of the TV structure in forward and reverse flow directions, with an initial Reynolds number (*Re*) of 200. The figure highlights the differences in the flow patterns and velocity distributions between the forward and reverse flow directions, demonstrating the effectiveness of the TV channel in rectifying fluid flow. Overall, the unique properties and design flexibility of the TV make it a promising technology for a wide range of microfluidic and macroscopic fluidic applications.

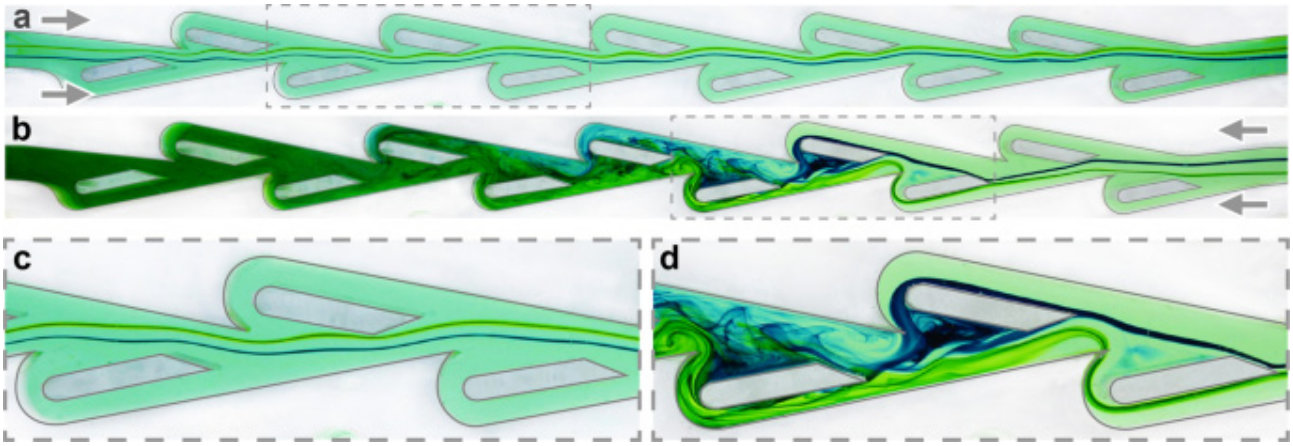

Figure 1. TV structure, visualized with green dye solutions in forward (**a**,**c**) and reverse (**b**,**d**) directions with a Reynolds number (*Re*) around 200. The flow is undisturbed in the forward direction (**a**,**c**). In the reverse direction, the flow resistance and mixing are predominant (**b**,**d**). *Reprinted from* [9] *under the Creative Commons license*.

Passive components, such as the TV channel, are acquiring increased attention in microfluidics and nanofluidics as they offer several advantages [17,18]. These components are cost-effective and can be easily integrated with sensors, making them more attractive for research and development. Passive components have disposable features, which are useful in applications where contamination or cross-contamination can cause issues. Another advantage of passive components is their smaller footprint, making them suitable for micro-scale devices. These components also have a simple control operation, which can help reduce complexity in microfluidic systems [19,20]. TVs have been studied for their use as passive components in microfluidics because of their straightforward design and effective fluidic control. In microfluidic devices, precise control over fluid flow is essential for numerous applications, including chemical and biological analysis, drug delivery, and microscale energy devices. TVs provide a straightforward and efficient solution for fluidic control as they can regulate flow with no external power or moving parts.

Although the TV has been known for over two decades, its integration into microfluidic devices is still relatively new. The limited number of research articles on TV in microfluidics indicates that the full potential of TV has yet to be explored [3]. We are motivated to investigate this gap profoundly and highlight the versatility and potential features of TV toward current technology trends for a wide range of applications, including lab on a chip, biochemical sensors, wearable devices, and green energy. Recent developments in microfluidics and nanofluidics, as the backbone of the miniaturized device, coupled with integrating sensors, have led to increased interest in passive components such as TV because of their cost effectiveness, disposability, and simple control operation of microfluidic devices. Despite the limited research (Figure 2), TV has shown promising results in various applications. For example, it can be used as a fluidic diode in a piston-based micropump to avoid flow back and limit the flow rate in particular devices, such as in DNA extraction where unidirectional flow is predominant to capture oligonucleotides in the solid phase membrane. Figure 2 shows the trend of research articles using the TV in their study. In addition, the TV can play a substantial role in the future microfluidics system with complex fluid management, comparable to the role of a diode in complex microelectronic circuits (Figure 3) and another electric-like component in the fluid devices [17] which greatly fit futuristic applications such as in wearable diagnostic tools and photovoltaic devices development. There is a need for a topical review of TV structures in microfluidics, including the state-of-the art of TV structure, performance parameters, diverse designs, and their derivatives, current trends, emerging applications, challenges of future development, and a summary. This review will provide a comprehensive understanding of the potential and limitations of TV in microfluidic systems and pave the way for further research in this area.

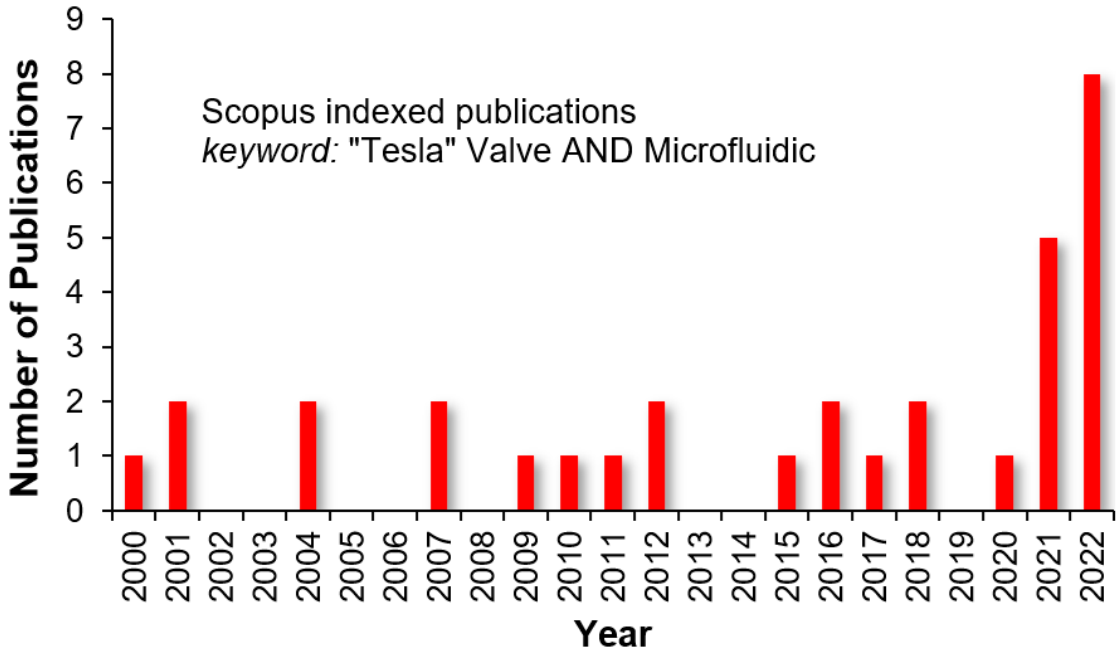

Figure 2. The trend of TV microfluidics publications, based on the Scopus index for the time range until 2022.

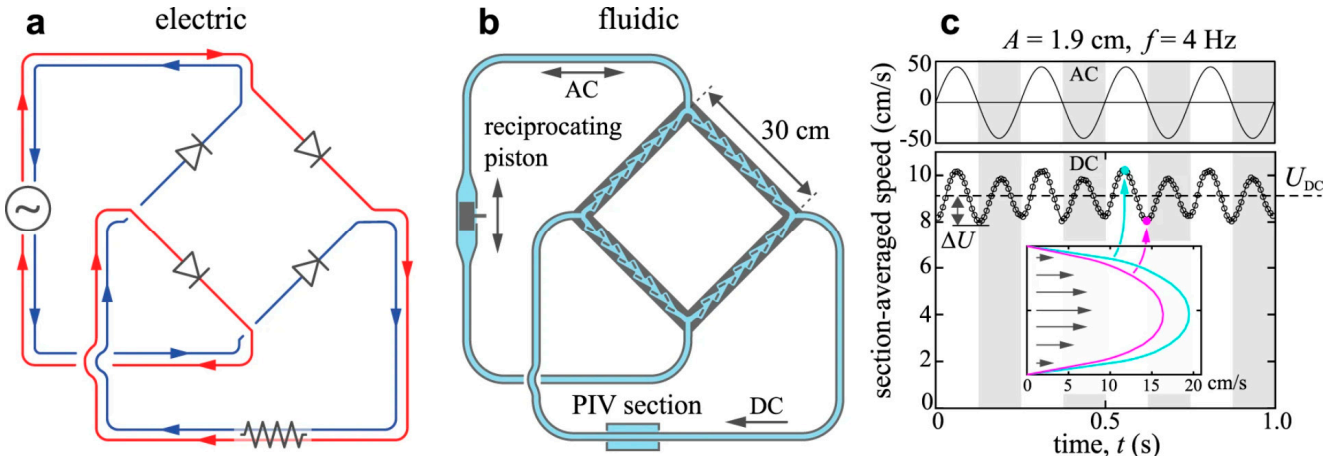

Figure 3. The equivalent circuit of electrical (**a**) and fluidic (**b**) rectifier using four TV channels. (**c**) The performance of fluidic rectifiers with comparable parameters in the electrical variables. *Reprinted from* [9] *under Creative Commons license*.

2. TV Performances

The flow rate of a TV refers to the amount of fluid that can pass through the valve per unit of time. This parameter is critical in evaluating the valve's performance since it determines the rate of fluid flow and, consequently, the efficiency of the valve. The pressure drop, on the other hand, refers to the decrease in pressure that occurs as fluid flows through the valve. The pressure drop is essential in determining the valve's energy efficiency as it determines the amount of energy required to move fluid through the valve. Finally, diodicity refers to the valve's ability to rectify fluid flow, allowing fluid to flow in one direction while restricting it in the opposite direction. This parameter is crucial in determining the valve's suitability for different applications since some applications require unidirectional flow while others require bidirectional flow. Therefore, by evaluating these parameters, one can determine the effectiveness of the TV and its suitability for different applications.

2.1. Flow Rate

A TV's flow rate (F) refers to the volume of fluid that can pass through it per unit of time. The typical flow rate in a TV depends on numerous factors, such as the valve's dimensions, the fluid properties, and the pressure difference across the valve. However, TVs have been shown to have higher flow rates than traditional check valves, especially at low Reynolds numbers. The flow rate can vary from a few milliliters per minute to several liters per minute, depending on the valve's design and the application. For example, in microfluidic applications, the flow rate may be as low as a few microliters per minute. In contrast, in industrial applications, it can be several liters per minute or even higher. The flow rate of a TV can be measured experimentally using flow sensors or calculated using computational fluid dynamics simulations. It can be expressed:

$$F = V/t \tag{1}$$

where F is the flow rate, V is the volume that passes the channel, and t is the time required to pass the volume of the liquid.

2.2. Pressure Drop

The pressure (P) drop across a TV refers to the difference in pressure between the inlet and outlet of the valve [16,21]. Typically, a high-pressure drop will be in the forward flow compared to the reverse flow. TV has been shown to have higher pressure drops than traditional check valves, which makes them suitable for fluidic rectification applications.

The pressure drop in a TV is typically lower than in a check valve, especially at low Reynolds numbers. In a traditional check valve, the pressure drop is primarily caused by the valve disc's weight and the spring tension that keeps it closed. This pressure drop can lead to a significant energy loss, especially in applications that require high flow rates.

On the other hand, TVs rely on the fluid's inherent properties to create the unidirectional flow. They do not have any moving parts, so the pressure drop is mainly because of the fluid's viscosity and the valve's geometric features. This results in a lower pressure drop and a more efficient flow compared to traditional check valves. The asymmetric geometry of the TV leads to a higher-pressure recovery, so the pressure after the valve is close to the inlet pressure compared to a check valve.

One way to define the efficiency in TV is the ratio of the pressure drop across the valve to the pressure drop in an equivalent straight channel. Both channels can be fabricated and connected in a single flow. This ratio is known as the pressure recovery factor (*PRF*) and can be expressed mathematically as:

$$PRF = P_v / P_s \tag{2}$$

where P_v is the pressure drop across the TV and P_s is the pressure drop in an equivalent straight channel of the same length and cross-sectional area. A higher *PRF* indicates better efficiency to reduce pressure drop.

2.3. Diodicity

The diodicity factor drives the performance of TV [9,13,16]. Diodicity refers to the directional flow behavior of a TV. When fluid flows in one direction through a TV, it experiences high resistance because of its complex geometry, creating a series of vortex-like flow structures that impede the fluid's progress [22]. However, when fluid flows in the opposite direction, it encounters much lower resistance and can easily flow through the valve. This directional flow behavior is like that of a diode in electronics, which allows current to flow in one direction but blocks it in the other. With TVs, this diodicity allows them to be used as passive components in microfluidic devices for controlling flow direction and preventing backflow. For example, TVs have been used as passive flow controllers in microfluidic mixers, where they help to ensure that fluids flow in the correct direction to achieve efficient mixing. They have also been used in microscale pumps to regulate fluid flow through the device and prevent backflow. Overall, the diodicity of TVs makes them a useful tool for controlling fluid flow in microfluidic devices, offering a simple and effective means of achieving directional flow control with no active components or external power sources. The diodicity of a TV can be expressed mathematically by the following equation:

$$D = P_b / P_f \tag{3}$$

where D is the diodicity, P_f is the pressure drop during forward flow, and P_b is the pressure drop during backward flow. The diodicity value typically ranges from one to two, where a value of one indicates that the valve has no diodicity and allows equal flow in both directions. A value larger than one indicates diodicity behavior, where flow occurs in only one direction. A higher diodicity value indicates a stronger preference for forward flow [16].

Reynold's number (*Re*) significantly influences the diodicity of the TV. The diodicity can work in practice only when the Reynolds number is larger than one. If the Reynolds number becomes close to unity, the flow is typically reversible, and the TV structure shows the same pressure drop in both directions. Nguyen et al. reported a strong correlation between *Re* and *Di* in the TV fluidics [9]. The higher the *Re*, the *Di* also increases. It means in the exceptionally low flow rate, the TV works as a fully reversible channel.

3. TV Design

Over the years, researchers have explored various applications of TVs in microfluidic devices. These applications have resulted in numerous designs of TV structures, which have been documented in the literature. In this topical review, the different TV designs have been classified into three categories: single-stage TV (STV), multistage TV (MSTV), and TV-derivative (TVD) structures. The STV design features a single valve, while the MSTV design comprises multiple valves that are arranged in series or parallel to increase their effectiveness. The TVD structures, on the other hand, are based on the principles of the TV but have been modified to improve their performance or suit specific applications. The categorization of TV designs is important in understanding the assorted options available for researchers and engineers when developing microfluidic devices that incorporate TVs.

3.1. Single-Stage TV (STV)

STV design is the most straightforward TV structure and is widely used in microfluidics devices because of its simplicity and ease of fabrication [15,23–32]. It comprises a non-periodic single tesla pattern connected to a microfluidic channel. The main advantage of this design is that it can be optimized with various angles and curvatures to achieve the desired flow characteristics [33]. For instance, the angle of the TV's sidewalls can be optimized to achieve a high diodicity while maintaining a low-pressure drop. The curvature of the structure can also be optimized to achieve a higher diodicity at low Reynolds numbers. Figure 4a–d shows examples of different STV designs in microfluidic channels. Lam et al. reported that the proposed STV on each channel was tested with an average inflow velocity of 0.1667 ms^{-1}, which is equivalent to a flow rate of 0.6 mL/min based on the valve's dimensions. Both forward and backward flow cases were tested, and the simulation showed that the pressure drop was higher for backward flow (440.9 kPa) than for forward flow (383 kPa). The TVs in the mixing module array effectively eliminated net backward flow generated from fluidic oscillation during active mechanical mixing [24]. Thompson et al. presented STV application in an oscillating heat pipe (OHP) and enhanced the reduction in thermal resistance by around 15–25%, depending on the power input. Their research suggested that TV is a promising approach to achieve circulatory flow rectification in an OHP, but further research is required to optimize the valve design, quantity, and alignment.

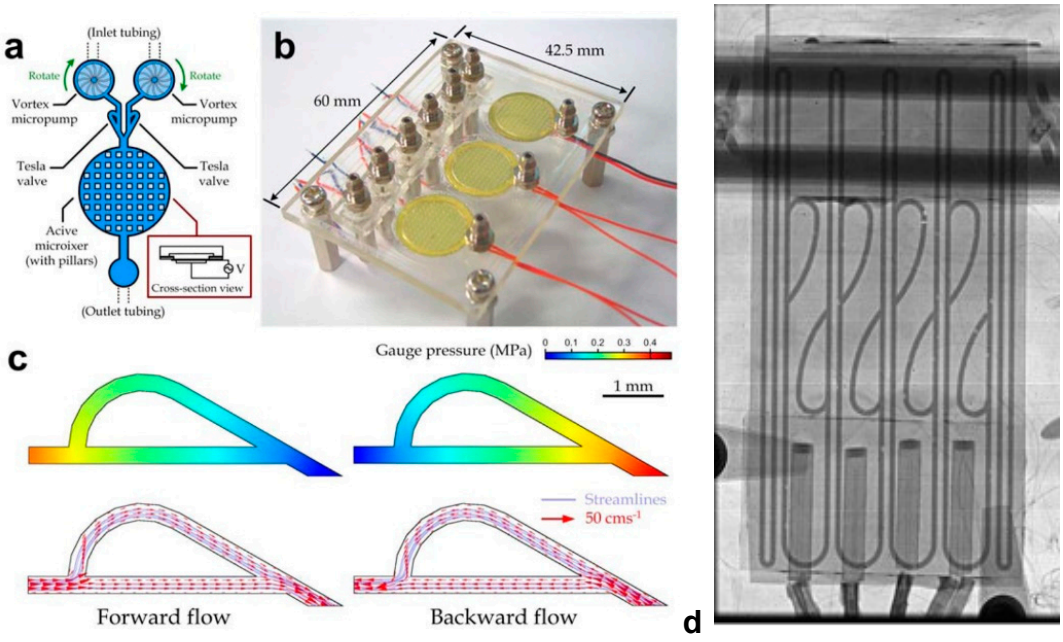

Figure 4. *Cont.*

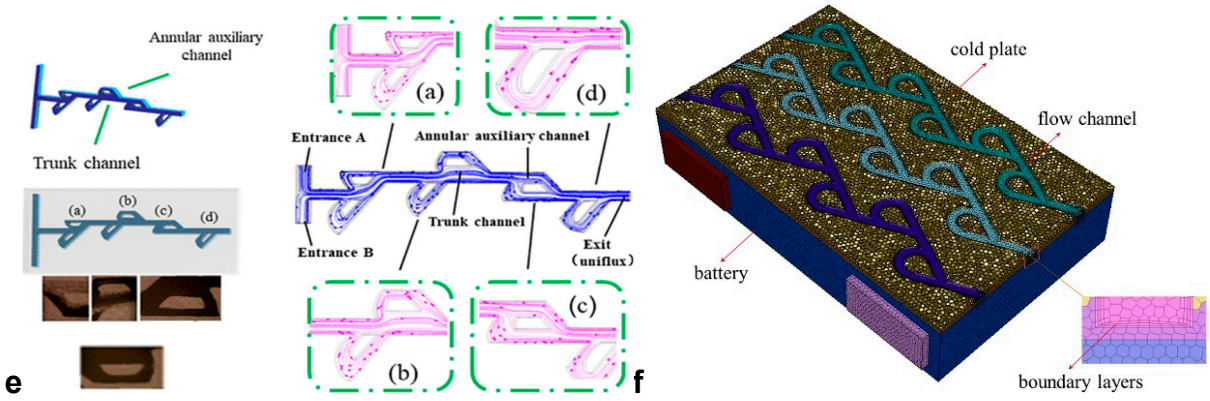

Figure 4. Single-stage TV structure for unidirectional flow components. (**a**) The single-stage TV structure in each inlet of the micromixer. (**b**) The digital integrated micromixer. (**c**) Two-dimensional simulations of pressure and velocity distribution of the fluidic in the TV structure. *Reprinted from* [24] *under Creative Commons license.* (**d**) The single-stage TV rectifier in the oscillating heat pipe. *Reprinted from* [34] *with permission, copyright © 2011 Elsevier.* (**e**) A multi-stage TV microchannel with an asymmetrical design in micromixer devices. *Reprinted from* [35] *under Creative Commons license.* (**f**) A multistage symmetrical TV design using high throughput channels. *Reprinted from* [36] *with permission, copyright © 2022 Elsevier*.

3.2. Multi-Stage TV (MSTV)

In contrast, the MSTV design comprises multiple single-stage TV structures connected in series [14,27,34,35,37–56]. Several MSTVs with optimized microfluidic dimensions have been reported in the literature, ranging from symmetrical to asymmetrical designs for different purposes [34]. For instance, an asymmetrical MSTV can enhance the diodicity performance in the forward direction while minimizing the pressure drop in the reverse direction. The multistage TV can be constructed with a single high-throughput channel or with multiple smaller channels for specific applications, such as particle separation or mixing [36,57]. Examples of different MSTV designs are shown in Figure 4e,f. Wang et al. presented flexible MSTV with a mold fabricated by 3D printing. The proposed MSTV micromixer has been found to enhance the mixing efficiency significantly to 87%. After conducting an experiment with four different groove structures and varying flow rates, it was observed that one type of the MSTV micromixer can achieve a mixing efficiency of up to 89% when the flow rate is 2 mL/min. These findings suggest that the TV design can efficiently improve the mixing process [34]. Lu et al. presented multichannel MSTV for cooling system in a battery. The results of the MSTV optimization indicate that the reverse TV-type channel cold plate is effective when the angle is set at 120°, the distance between adjacent TVs is 23.1 mm, the distance between adjacent channels is 28 mm and the coolant inlet velocity is 0.83 m/s. This configuration balances heat exchange performance and energy consumption, while keeping the maximum battery temperature under 30.5 °C and minimizing the pressure drop across the channels [36]. Overall, the multistage TV design offers higher diodicity performance compared to the single-stage TV design, making it more suitable for complex microfluidic applications [58].

3.3. TV Derivative Design (TVD)

The third design is the TV derivatives (TVD), inspired by the original TV microchannel and its basic principle with improvised shapes or stages [18,22,41,59–61]. An example of the design and fabrication process of the TVD is depicted in Figure 5 [18]. Bohm et al. presented TVD with optimized structures that exhibit a diodicity of 1.8 even at low flow rates of 20 µL/s, which is equivalent to a Reynolds number of 36. Lin et al. demonstrated a computational algorithm to construct a TVD geometry for a three-dimensional (3D) printing process [22]. With the massive growth of computer-aided design (CAD) techniques, TVD designs were also reported to predict the design's performance in the experimental analysis of the tested device. Lin et al. reported TVD to maximize diodicity, with a

principle to minimize forward dissipation and maximize reverse dissipation. Although previous research has focused on minimizing dissipation for topology optimization of fluids, maximizing dissipation poses difficulties because of the small, mesh-dependent flow channels and the numerical preference for artificial flow in solid regions. To overcome these challenges, they demonstrate a projection method to control the minimum length scale of channels, and an extra penalty term is introduced to regulate the flow through intermediate porosities. Various solutions are proposed, and one of them is fabricated by 3D printing and experimentally tested to demonstrate its diode-like behavior [22].

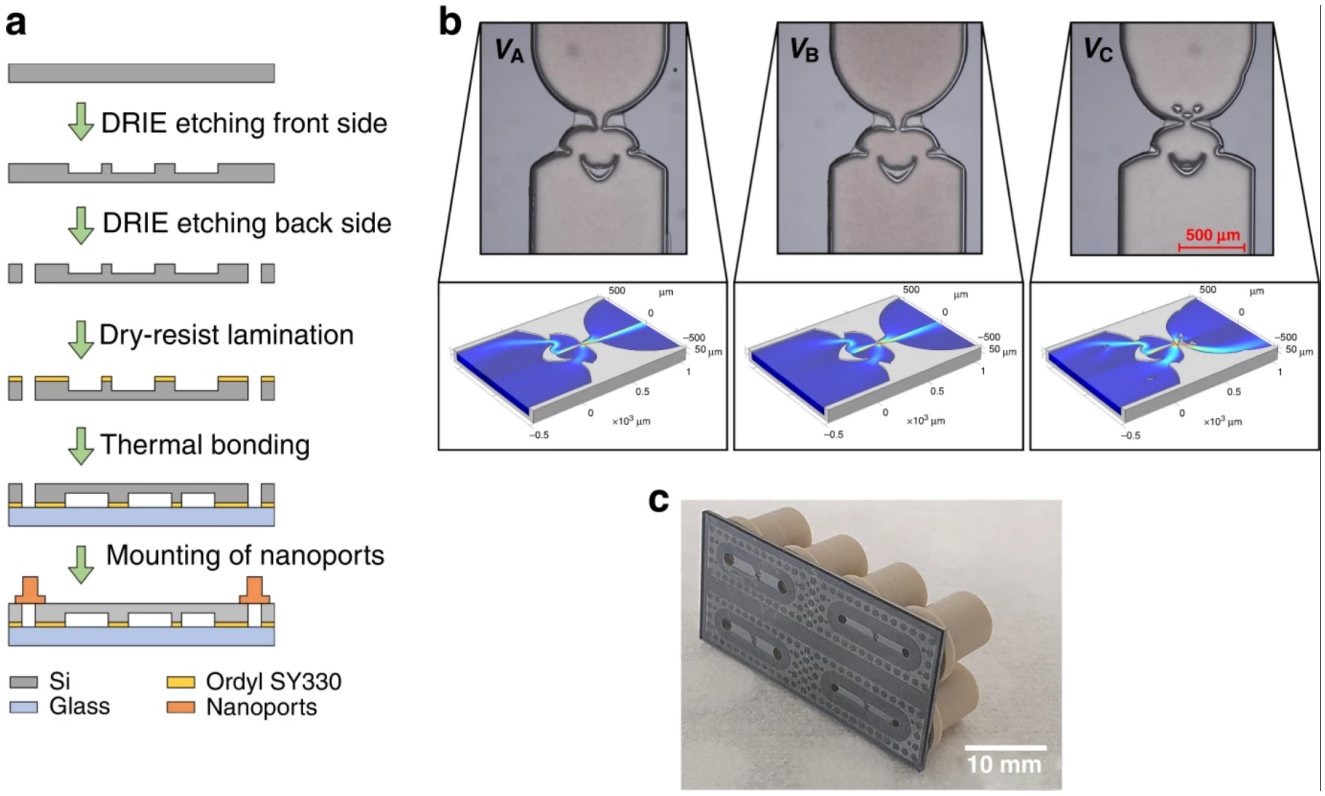

Figure 5. The TV derivative design and its fabrication process. (**a**) Lithography and bonding process of the TV derivative microfluidics. (**b**) A computational fluid dynamic (CFD) simulation optimizes the TV channel. (**c**) The microfluidics image with TV-derivative design. *Reprinted from* [18] *under Creative Commons license.*

Shalabi et al. successfully performed the sealing of the capacitive sensor unit using a TVD design. The TVs were integrated with dead-end channels to control the seal and release flow from the pressure response [62]. The TV in their research uses teardrop-shaped loops to create a one-way flow of fluids and has been commonly used in microfluidic devices. In this study, they used this valve's one-way function as an approach to enable the microfabrication of a device. Using a vapor-phase thin-film deposition technique, they used on-chip micro-Tesla valves with unique channel structures to release and seal the cavity [62].

4. Recent Trends and Applications

According to the literature review on TV microchannels, applications can be categorized in several areas: unidirectional flow components in microdevices, micromixers, cooling or heating microsystems, and renewable energy devices, such as battery and fuel cell applications.

4.1. Unidirectional Flow Components

The TV microchannels were used in the forward modes for unidirectional flow components in the microdevices. The principal aim of this configuration is to avoid the backflow of the fluids. The straightforward application in this part is in the micropump devices [23,35,39]. Yao et al. demonstrated the TV microchannel for the piezoelectric pump. A single-stage TV is in the inlet and outlet of the piezoelectric house, respectively, for a reverse diversion channel [31]. Not only that, but notable research also reported on the application of TV microfluidics for sealing the collected sweat at wearable devices and integrating it into a colorimetry sensor, as depicted in Figure 6. The study proposed utilization of the Tesla microvalve to prevent reflux and outside air and to apply it to a wearable sweat collecting device. Holding to the concept that TV generates diodicity at low flow rates, a forward and reverse TV was employed at the inlet and outlet of the sweat collector to reduce the reflux and external oxygen. The study concluded that paper-based glucose and pH sensing in a wearable device with portable photoelectric detector was the potential for colorimetric analysis. The long-lasting design of the microfluidic sweat acquisition chip offers new perspectives for the design of wearable sensors and detection approaches [51].

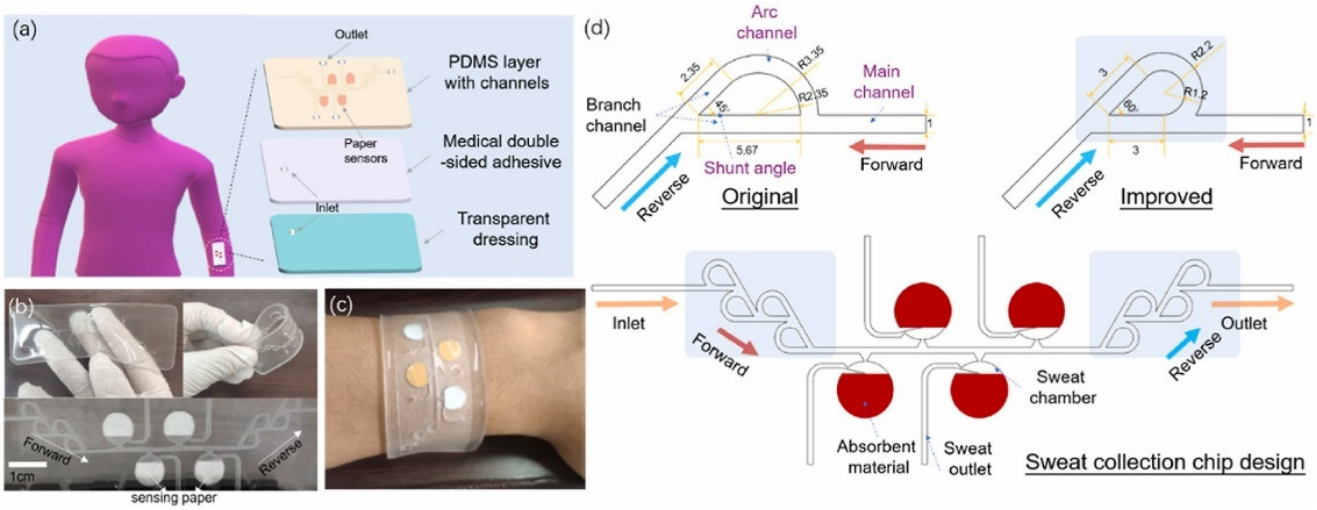

Figure 6. A proof-of-concept of the TV microchannels for sweat collection in a wearable device. (**a**) The structure of the sweat collection devices. (**b**) the TV microchannels and the paper sensing components. (**c**) The sweat collector device with detected colorimetry. (**d**) The primary mechanism of the sweat collection chip. *Reprinted with permission from* [51] *copyright © 2022 Elsevier*.

Shalabi et al. proved that TV-inspired microchannels exhibit an excellent ability to manage a responsive capacitive sensor's release and sealing mechanisms and to protect the sensing membrane, as depicted in Figure 7a [62]. The cavity was completely clear from any sealants; therefore, a facile ohmic contact was created between the membrane and the individual switch. The sacrificial layer was dissolved as the membrane was released toward the shortest channel in the opposite direction of the TV. The cavity was sealed with Parylene C that blocked the channels. The parylene molecules in the vapor phase flowed into the channel, passing through the multiple TV and returned to the main channel facing the forward molecular movement. As a result, parylene trapping by the valves and deposition on to the channel wall hindering the forward flow occurred. In between the valves, "sponges" or dead-end paths were added to enlarge the inner surface area in the channel. They also facilitated the adhesion of the parylene that had a tendency to leave the TV to the channel wall before the cavity. A complete blockage of the microchannel to attain optimized vacuum sealing at the sensor cavity was realized through this mechanism [62].

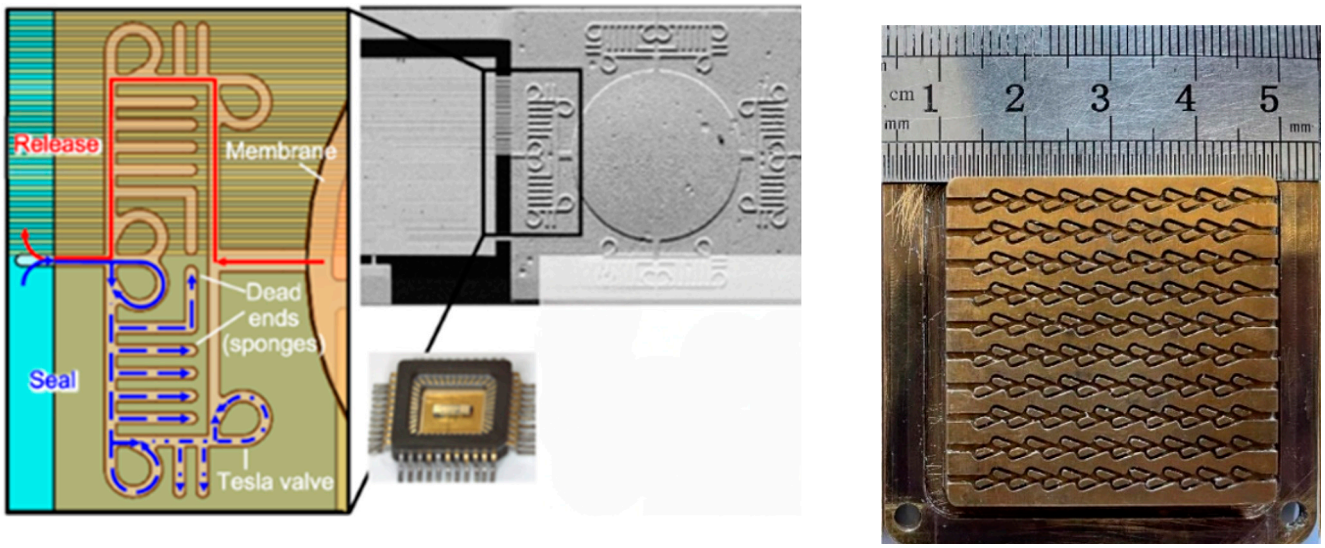

(**a**) (**b**)

Figure 7. The (**a**) TV microchannel for release and sealing management in capacitive sensor protection. *Reprinted from* [62] *under Creative Commons license.* (**b**) The high throughout TV microfluidics for flow boiling system in electronic devices. *Reprinted with permission from* [57] *copyright © 2023 Elsevier*.

4.2. Micromixer

Micromixer components are a tremendous trend in the microfluidics field. Two or more solutions from inlets were mixed in microchannels and resulted in a single outlet. One of the important parameters for micromixer device is the degree of mixing (δm); this can be expressed as:

$$\delta m = 1 - (\delta_b / \delta_{max}) \quad (4)$$

where δ_b is the standard deviation of the volumetric flow and δ_{max} is the maximum value of δ_b, which is obtained for two completely separated flows. Consequently, the δm value will be between 0 and 1 [11]. Another term, mixing efficiency, sometimes is used interchangeably with the degree of mixing to evaluate the micromixer performance. Mixing efficiency is given in percentage value between 0 and 100%.

Micromixer channels application using TV microfluidics were reported in the literature [10,11,34,55,63–65]. The micromixer harnesses the channel's reverse flow and enhances the mixing in the conjunction channels, especially using multistage TV (Figure 1b,d). Wang et al. reported, under a specific condition, the mixing efficiency using MSTV can be up to 99% [64]. The enhanced mixing efficiency can be attributed to the liquid passing through the diversion port, which forms two separate liquid streams that subsequently remix and generate secondary flow and local vortex. The alteration of fluid direction as it flows through the bend results in the collision of the two liquids, significantly improving the mixing efficiency.

One of the diluted materials for mixing solutions in TV devices is nanoparticles [50,63]. Liosis et al. presented a simulated study of Fe3O4 micromixer using TV. The simulations focused on nanoparticle inlet rates and velocity ratios, with the forward flow chosen for the analysis. The simulations' visualizations indicated that uniform nanoparticle distribution was achieved in the micromixer at a velocity ratio of $Vp/Vc = 20$. The micromixer's mixing efficiency was found to be 63% at $Re = 0.62$ with two Tesla units and nanoparticles occupied a significant portion of the micromixer's height and width near the exit. Inlet rates were identified as crucial in determining mixing efficiency for lower velocity ratios. The velocity ratio was identified as the decisive factor in mixing efficiency, with increased value resulting in improved performance. Although the nanoparticle diameter's increase from 13.5 to 27 nm had no significant effect on the mixing efficiency, further simulations are required

to test for different diameters [63]. Michalska et al. demonstrated the using of TV for mixing NiO nanoparticles for organic solar cell fabrication [50]. The approach involves using NiO nanoparticles (NPs) modified with either 4-hydroxy benzoic acid (HBA) or trimethyloxonium tetrafluoroborate (Me3OBF4) ligands in combination with a Tesla-valve microfluidic mixer. The resulting NP dispersions and thin films are characterized using various techniques, including optical, structural, thermal, chemical, and electrical methods. The ligand-exchanged NiO NPs retain their optical and structural properties, similar to those with native long-chained aliphatic ligands. However, the ligand modified NiO thin films exhibit reduced surface energy and increased hole mobilities [50].

Wang et al. with the MSTV structures (Figure 4e) demonstrated the mixing application for food science [34]. In the experiment conducted using a TV micromixer, the effect of purple litmus reagent and white vinegar was presented. It was observed that the final solution formed was red, indicating the acidic nature of white vinegar. The gray value was analyzed and the mixing efficiency was calculated, showing that as the mixing time increased, the mixing efficiency gradually improved. The highest mixing efficiency of 0.893 was observed in a particular location. The results were further analyzed using fitting and the value of R^2 was found to be 0.986, indicating a linear increase in mixing efficiency as time went by [34].

Guo et al. developed a 3D micromixer with four integrated TVs to mix the solutions uniformly [55]. To evaluate the performance of the micromixer, numerical, simulations and experiments were conducted. The study demonstrated that repeated separation and solution integration in TV triggered planar transverse diffusion, which enhanced the mixing process. Subsequently, turning the two mixing units, specifically at the connections, disturbed the flow, which prolonged and deformed the contact interfaces. This phenomenon leads to the mixing efficiency enhancement. As the flow rates and polymer concentrations were adjusted, a mixing efficiency of >86.96% with flow rates over 500 µL/min (Re = 1.1), and >89.98% for viscoelastic solutions with PEO concentrations ranging from 0 to 500 ppm (Re = 0.7–1.3) were achieved. This micromixing protocol showed outstanding results in chitosan nanoparticles synthesis (diameter ranging from 40 to 190 nm). This micromixing method was more effective in yielding a more uniform and narrow size distribution of the particle than the typical chemical route of nanoparticle synthesis [55].

4.3. Thermal Manipulation System

Recently published works denoted the potential of TV microchannels for the cooling system and thermal manipulation [36,56,57,66,67]. Several researchers reported a cooling system for lithium-ion batteries using a TV microchannel [36,49,67]. One of the heatsink structures with parallel multistage TV microchannels has been shown in Figure 4f. Because of its bifurcated structure, the TV-type channel cold plate had superior heat exchange performance and temperature uniformity, especially under strong heat flux. At a flow velocity of 0.8 m/s, the maximum temperature ($Tmax$) of the RTV-type channel was reduced by 3.4 °C and 4.4 °C compared to the FTV-type and Z-type, respectively, at the expense of pressure drop (ΔP). Furthermore, the temperature difference (ΔT) was also lowered by 32% and 39%, respectively. Through multi-objective optimization, an RTV-type channel cold plate with α of 120°, L of 23.1 mm, B of 28 mm, and v of 0.83 m/s achieved a good balance between heat exchange performance and energy consumption. The optimized cooling system maintained a maximum battery temperature below 30.5 °C while keeping a low channel pressure drop. The corresponding values for $Tmax$, ΔT, and ΔP were 30.478 °C, 5.486 °C, and 9475 Pa, respectively [36].

On the other hand, the TV structures were used for heat-pipe applications [26,28,58,68]. In such applications, the TV channels control circulatory flow and block the reversed flow at higher heat inputs [69]. Rui et al. proposed a TV microchannel to control the flow of heat dissipation for thermal management in electronic devices [57]. The fabricated structure is presented in Figure 7b. The study compares two microchannels: with MCTV

and microchannel with sector bump (MCSB). The study examined the impact of mass flow rate, inlet temperature, and heat flux on flow boiling in two microchannel structures and identified the more effective structure for heat dissipation and cooling systems. The findings indicate that both microchannels provide stable boiling states and experience pressure drop fluctuations of 0.8% to 3.9%. However, the MCSB structure demonstrated a 45% higher heat transfer coefficient and a 25% lower pressure drop than the MCTV structure on average. The MCSB structure had a larger effective heat flux for the onset of nucleate boiling (ONB) compared with the MCTV structure. Overall, the study concludes that the MCSB structure has superior thermal-hydraulic performance in flow boiling processes than the MCTV structure, and a proper correlation has been selected and adjusted to predict the heat transfer coefficient of both microchannels [57].

4.4. Energy Devices

Currently, more reports apply TV microchannels to control the fluidic flow on the energy devices, such as batteries [36,49,67], fuel cells [14,15,44,70], and bioreactors [61]. As described in the previous subsection, the TV microchannels in battery devices were primarily used as the cooling system to dissipate the heat from the battery during operation effectively. TV microchannels were proposed in fuel cell devices to control the flow from hydrogen decompression [14,15,44]. An interesting study on the hydrogen flow through the MSTV during the decompression process in a fuel cell was demonstrated by Qian and coworkers. They focused on comprehending the velocity, temperature, and pressure characteristics under different MSTVs. The setup included the turbulent flow with the inlet and outlet pressure ratio ranging from 1.05 to 2.4. It was revealed that when the hydrogen was flowing toward the outlet, pressure reduction and minimum pressure recovery occurred. After the liquid passing at the intersection of the bend and straight channels at each stage, low-pressure, low-temperature regions, and jet impingement were likely to happen. In the last stage, minimum pressure and maximum velocity were observed simultaneously. When a small stage number was applied. The velocity surpassed the local acoustic speed in a high-pressure ratio. A power law had been associated with the stage number and pressure ratio in the MSTV flow rate. These findings can aid designing and selecting Tesla valves and the number of stages required for hydrogen fuel cell applications. Using pressure-reducing valves can be minimized [14].

Lu et al. attested to the potential use of multistage TV for a proton exchange membrane fuel cell (PEMFC). MSTV channels outperform the conventional serpentine flow field (CSFF) and conventional parallel flow field (CPFF) in terms of the oxygen mass fraction in the cathode GDL/CL interface (Figure 8) [70]. This research group demonstrated numerical and experimental analyses to learn the transport characteristics of the direction correlated MSTV flow field. They emphasized to discriminate the transport characteristics of the forward (MSTV-F) and reverse flow (MSTV-R) of MSTV. A simulation study confirmed the versatility of the MSTV where in both MSTV-R and MSTV-F, the velocity flow surpassed the CPFF by 24.17% and 13.61%, respectively, triggering the higher reactant diffusion that moved toward the gas diffusion layer (GDL). There was a relatively lighter drop in pressure in MSTV-R and MSTV-F in CSFF and a higher net power density than in both CPFF and CSFF. To optimize the net power regardless of the conditions, the inlet commutation strategy had been regarded as a potential solution. More homogenous current density distribution of MSTV-R flow field was typical in a high-load chip. This is essential since this behavior could attenuate the local fuel starvation in PEMFC.

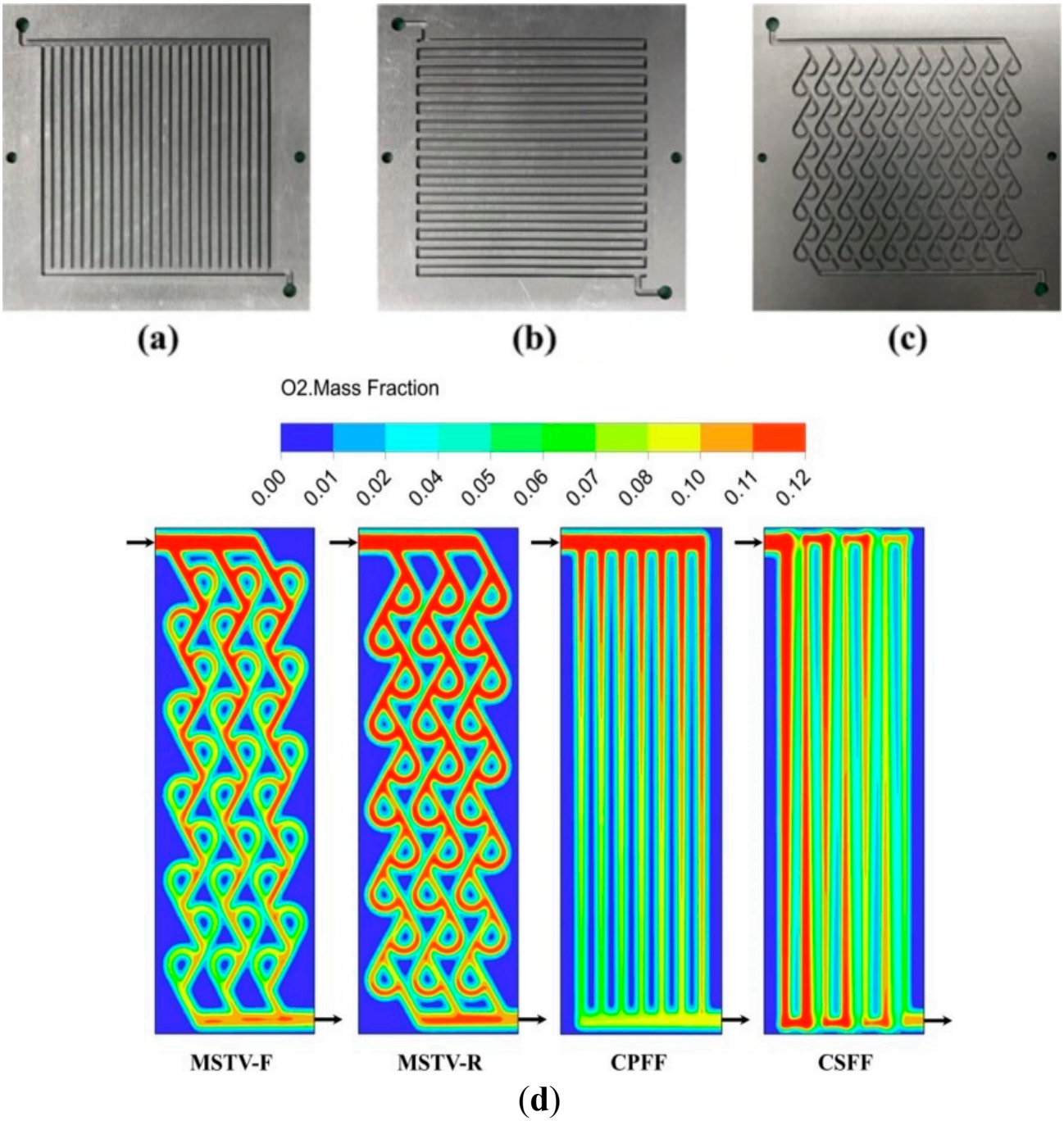

Figure 8. The multistage TV microchannels in the proton's cathode exchange membrane fuel cell (PEMFC). (**a**–**c**) Fabricated MSTV CPFF and CSFF structures. (**d**) Simulated results show a higher fraction of oxygen both in forward and reverse flow (marked as MSTV-R and MSTV-F) compared to the conventional parallel flow field (CPFF) and conventional serpentine flow field (CSFF). *Reprinted with permission from* [70] *copyright © 2023 Elsevier*.

4.5. Lab on a Chip and Chemosensors

TV implementation in biomedical devices is a huge potential in the near future. The reported TVs in this area until this review is written are still limited. Shi et al. presented the TV devices as a main component in a wearable device for sweat analysis, as we have described in Figure 6 [51]. This proof of concept is a critical milestone for the further development of lab-on-a-chip applications using TV. The MSTV structure, presented by

Wang et al., as depicted in Figure 4e, demonstrated the application of a micromixer in food science for mixing the purple litmus reagent and white vinegar [34].

The world health organization (WHO) defined the requirement of biochemical sensor to be ASSURED: affordable, sensitive, specific, user-friendly, rapid and robust, equipment-free, and deliverable to end users [20]. As a passive component that rely on the design topology without any moving parts, a TV based channel will be compatible with the aspect of affordability because of the low-cost fabrication, robustness, and equipment free to control the valves because there are no actuators.

Fully disposable sample preparation and labeling on a chip as presented by Prabowo et al. [69,71] is also potentially developed using TV for the microchannels to enhance mixing and avoid back flow when capillarity attraction is saturated. Another potency of TV is in the organ on chip devices [72,73]. TV can mimic the liver on a chip to control a stable flow of fluid through the liver tissue, allowing for the study of drug metabolism and toxicity such as that introduced in the previous literature [74,75].

Besides these applications, TV can also be used for other biomedical purposes such as drug delivery, cell sorting, and biosensing [76]. TV can offer precise control of fluid flow and direction in microfluidic systems, enabling accurate delivery of drugs or biomolecules to target cells or tissues. TV can also facilitate the separation and isolation of different cells based on their physical or biochemical properties, such as size, shape, density, or affinity. TV can also enhance the sensitivity and specificity of biosensors by regulating the transport and reaction of analyte and reagents in microchannels. These advantages of TV make it a promising technology for biomedical devices that require high performance and functionality.

Moreover, for chemosensor applications, the ion trapping microfluidics [77–79] are promising to implement the TV for the flow management of the sample. TV can control the certain flow rate and the direction for the specific sample flow. For specific methods such as ion concentration polarization (ICP), ion selective polymers can be combined with the TV channels to manipulate ion trapping or particle trapping because of charge differentiation [77,80,81].

5. Summary and Outlook

The application of TV microchannels has grown significantly because of their unique features, including diodicity flow and ease of fabrication. The versatility of TV microchannels has enabled its use in a wide range of fields, such as wearable devices, micropumps, micromixers, and thermal control, among others. The ability to fabricate TV microchannels through top-down methods has eliminated the need for further integration or component alignment, making it a more cost-effective solution. The diodicity flow in passive components has also paved the way for numerous practical applications. As a result, TV microchannels have become a popular choice for researchers and designers across various fields.

Over the last two years, there has been a surge in research focused on TV microchannels in microfluidic devices for liquid or gas samples. These microchannels have been used in sample preparation chips, wearable devices, and renewable energy devices. Table 1 and Scheme 2 summarize the pivotal features of TV fluidics, which highlight the importance of these microchannels in various fields. As the interest in artificial intelligence continues to skyrocket, the evolution and optimization of novel TV topology will become another crucial step toward the future of automation and the digitalization of analytical systems. With the development of an algorithm that enables TV derivative designing and its optimization for specific analysis targets, the potential applications of TV microchannels in various fields will only continue to expand. However, one limitation of TV as a passive component in fluidics is how to stop the fluidic flow effectively. Although fluidic switching in passive microchannels poses a challenge, researchers are optimistic about developing potential solutions to address this issue.

Table 1. The list of TV fluidics report, with its findings and potential applications.

No.	TV Structure	Technical Remarks	Finding	Potential Applications	Ref.
1	MSTV	Original design, patented	Detracting from its practical value and significantly adding to its manufacturing and maintenance cost.	Machinery	[1]
2	STV	3D simulation, high-fidelity models	Validation of compact model behavior in SPICE and SABER	Microfluidics, micropump, and microsystem	[27]
3	STV	Fabricated micropump	Optimized structure and its validation	Micropump	[23]
4	STV	Digitally controlled microfluidics	Real-time fluid mixing and concentration regulation with the mixing module array	Micromixer	[24]
5	STV	Design and implementation	Novel TV in pulsating heat pipes	PHP	[26]
6	STV	Numerical study	Hydrogen decompression at the reverse flow	Fuel cell devices	[15]
7	STV	Topology optimization	Reconstructed TV topology	Optimized TV design	[45]
8	STV	CFD simulation	TV in the natural circulation loop	Supercritical CO_2 circulation	[30,66]
9	STV	Valveless piezoelectric pump	Suppression enhancement of the backflow	Micropump	[31]
10	STV	TV inlet of the combustor	Suppression of pressure feedback of the rotating detonation combustor	Combustor	[32]
11	MSTV	Numerical study	Lower maximum flow rate for all range of operating frequencies	Valveless micropump	[39]
12	MSTV	An integrated check valve at OHP	Improved thermal circulation at OHP	Thermal flow control	[28,58]
13	MSTV	CFD simulation	An order-of-magnitude denser gaseous beam of molecules	Gas delivery system	[48]
14	MSTV	Numerical analysis	Enhancement of heat transfer in the proposed cooling system	Li-ion battery	[49]
15	MSTV	Micromixer for ligand-engineered NiO nanoparticles	Facile fabrication of low temperature hole-transporting layers in perovskite solar cells	Perovskite solar cell	[50]
16	MSTV	3D printed devices	Designed and fabricated turbine fluidic pump using DLP-based 3D printing.	Micropump, Lab-on-a-chip	[40]
17	MSTV	Numerical modeling	Volumetric efficiencies enhancement than nozzle–diffuser elements.	Micropump	[35]
18	MSTV	Fluidic rectifier circuit	Comparable electric and fluidic rectifier circuit	Mixing and pumping	[9,13]
19	MSTV	3D printed devices	Mixing efficiency improvement up to 87%	Micromixer	[34]
20	MSTV	TV in flexible microfluidic	Integration of sweat collector and colorimetric sensor	Wearable devices	[51]
21	MSTV	TV in the cold plate	TV reverse flow causes fluid mixing and vortices effectively	Cold plate system	[53]
22	MSTV	The vibroconveyor and the Tesla valve	Vertical pulse elevator, independent from frictional interactions, torque less	Pulse elevator of inert materials	[54]

Table 1. *Cont.*

No.	TV Structure	Technical Remarks	Finding	Potential Applications	Ref.
23	MSTV	Novel 3D TV micromixer	Mixing efficiency: 86.96% at *Re* = 1.1	Micromixer for chitosan NP	[55]
24	MSTV	Fabricated TV microfluidics	Fabrication of TV using femtosecond bursts	Microfluidics device	[82]
25	MSTV	Numerical optimization	The reverse Tesla valve balances heat exchange performance and energy consumption	Battery cold plate	[36]
26	MSTV	Reversed TV	Enhanced fluid mixing using a reversed flow	Micromixer	[11]
27	MSTV	Numerical study	Heat transfer area improves around 94–112%	Heatsink	[26]
28	MSTV	Proton exchange membrane	Peak net power of MSTV flow field for reverse and forward flow can be increased by 19.89% and 3.90%	Fuel cell	[70]
29	MSTV	MSTV combination with phase change material	Reduction in the total energy consumption for coolant circulation by 79.9%	Battery	[67]
30	MSTV	MSTV and MSCB	MCSB has superior thermal-hydraulic performance in the flow boiling process than MCTV	Thermal hydraulic	[57]
31	TVD	3D printed TVD	Topology optimization	Novel TV design	[30]
32	TVD	CFD simulation	3D design and optimized TVD	Novel TV design	[60]
33	TVD	TV baffles in bioreactor	Photochemical efficiency enhancement	Photobioreactor	[61]
34	TVD	Fabrication optimized TVD	Diodicity: 1.8 at *Re*: 36	Novel TV design	[18]
35	TVD	Combination of TV and dead-end channels	Sealed and released control of the main sensor region	Capacitive sensor	[62]
36	TVD	Topology optimization	Topology optimization incorporating Pareto frontier exploration	Novel TV design	[59]
37	TVD	Acustofluidic micromixer	Efficient mixing across a broad range of flow rates (20–2000 μL/min)	Micromixer	[83]
38	TVD	Sharp edge acoustofluidic	Stable flow rates 8 μL/min (~76 Pa)	Acoustofluidic pump	[84]
39	TVD	3D PDMS microchannel	Mixing efficiency up to 90% at *Re* 0.6.	Micromixer	[85]

STV: single-stage tesla valve; MSTV: multistage tesla valve; TVD: Tesla valve derivative; OHP: oscillating heat pipes; PHP: pulsating heat pipes; CFD: computational fluids dynamic; *Re*: Reynolds number; NP: nanoparticles; MSCB: microchannel with sector bump; 3D: three dimensional; PDMS: Polydimethylsiloxane.

The prominent analogy between TV as the fluidic diode and a passive device with the fluidic circuit should be explored profoundly. The transistor fluidic might become a milestone for next-generation fluidic technology. The transistor fluidic is a passive component that operates similarly to a field-effect transistor in electronics. It is composed of a channel, source, drain, and gate, and it can act as a switch for fluidic flow. If this technology can be developed further, it could lead to significant advancements in microfluidics and expand the range of potential applications even further. In the future, the TV passive component will be significantly important for biomedical applications, such as biochemical sample preparation chips, lab-on-a-chip devices, clinical sample treatment devices, and organ-on-chip applications.

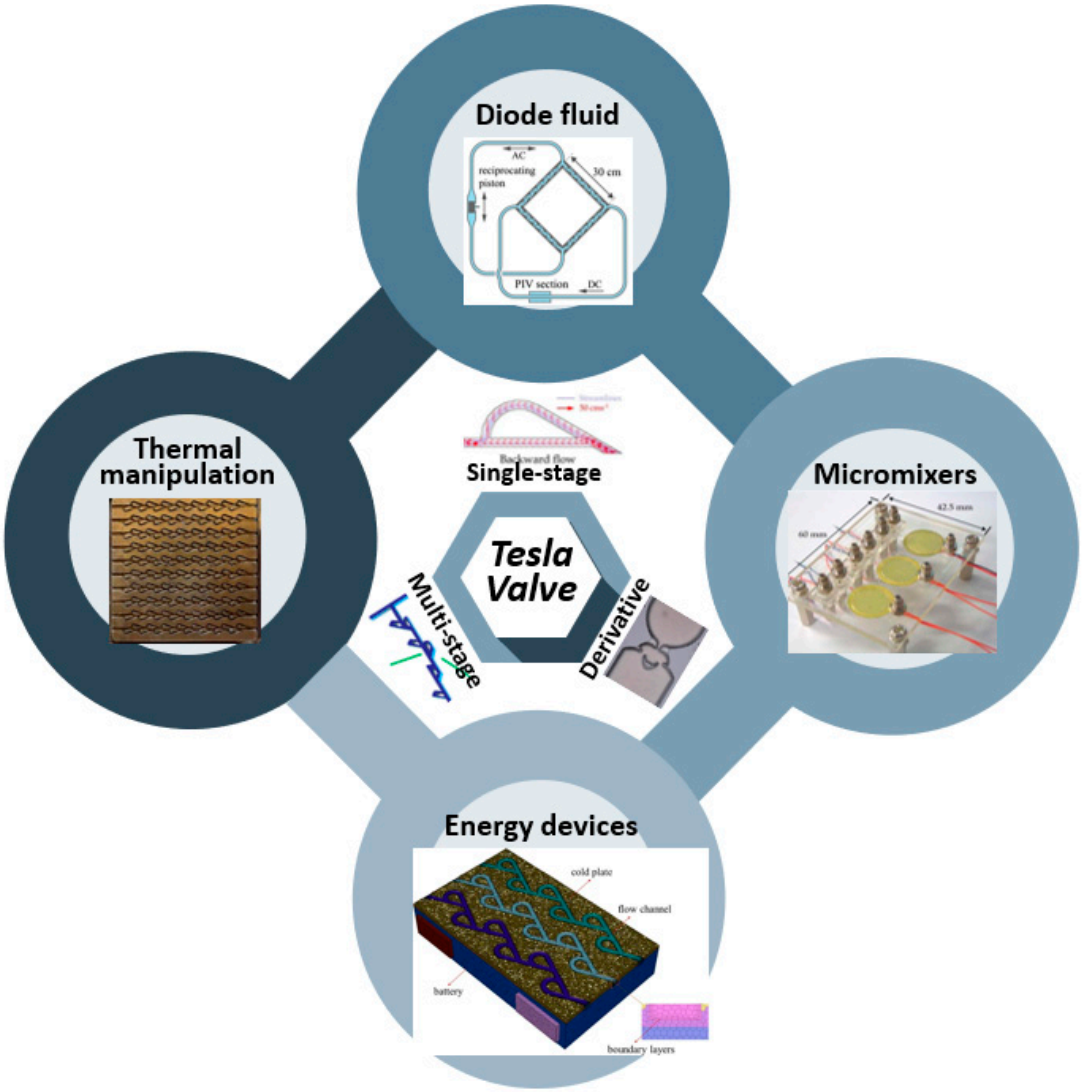

Scheme 2. Summary of TV structures and its applications.

Passive and active valves are two types of valves that can be used for fluid control in various applications. Passive valves rely on the structure or the chemical properties of the device to regulate the fluid flow, while active valves use external inputs, such as mechanical or electrical operation, to manipulate the fluid flow. Passive valves are usually simpler and cheaper to manufacture, but they have limited control over the response speed and accuracy of the fluid. Active valves can provide more precise and flexible control over the fluid, but they require additional power sources and components.

The comparison between passive and active valves, such as TV and diaphragm valves, includes Reynold's number, viscosity, fluid velocity, channel dimension, hydrophilicity of the channel, pH solutions, and channel length. These variables can affect the performance and efficiency of a different type of valve. Therefore, it is important to consider the specific requirements and conditions of each application when choosing between passive and active valves.

Author Contributions: Conceptualization, B.A.P.; methodology, B.A.P.; investigation, B.A.P. and A.P.; writing—original draft preparation, B.A.P.; writing—review and editing, B.A.P. and A.P.; visualization, B.A.P.; All authors have read and agreed to the published version of the manuscript.

Funding: This research received no specific grant from public, commercial, or not-for-profit funding agencies.

Institutional Review Board Statement: Not applicable.

Informed Consent Statement: Not applicable.

Data Availability Statement: All data supporting this study's findings are included in the article. Figures presented in the article are reprinted under the Creative Common License or with written permission from the respective publisher.

Acknowledgments: The author declares that they have no known competing financial interests or personal relationships that could have appeared to influence the work reported in this paper.

Conflicts of Interest: The authors declare no conflict of interest.

References

1. Tesla, N. Valvular Conduit. U.S. Patent 1329559A, 3 February 1920.
2. Tesla, N. Method of Obtaining Direct from Alternating Currents. U.S. Patent 413353A, 22 October 1889.
3. Stith, D. The Tesla Valve—A Fluidic Diode. *Phys. Teach.* **2019**, *57*, 201. [CrossRef]
4. Matthew Sparkes Century—Old Water Valve Invented by Nikola Tesla Could Have Modern Use. Available online: https://www.newscientist.com/article/2277794-century-old-water-valve-invented-by-nikola-tesla-could-have-modern-use/ (accessed on 12 January 2023).
5. Leigh, S.C.; Summers, A.P.; Hoffmann, S.L.; German, D.P. Shark Spiral Intestines May Operate as Tesla Valves. *Proc. R. Soc. B Biol. Sci.* **2021**, *288*, 20211359. [CrossRef] [PubMed]
6. Palecek, A. Shark Bellies Flow like Tesla Valves. *J. Exp. Biol.* **2021**, *224*, JEB237339. [CrossRef]
7. Farmer, C.G.; Cieri, R.L.; Pei, S. A Tesla Valve in a Turtle Lung. *Integr. Comp. Biol.* **2019**, *59*, E67.
8. Farmer, C.G.; Cieri, R.L.; Pei, S. A Tesla Valve in a Turtle Lung: Using Virtual Reality to Understand and to Communicate Complex Structure-Function Relationships. *J. Morphol.* **2019**, *280*, S70.
9. Nguyen, Q.M.; Abouezzi, J.; Ristroph, L. Early Turbulence and Pulsatile Flows Enhance Diodicity of Tesla's Macrofluidic Valve. *Nat. Commun.* **2021**, *12*, 2884. [CrossRef]
10. Wang, C.-T.; Chen, Y.-M.; Hong, P.-A.; Wang, Y.-T. Tesla Valves in Micromixers. *Int. J. Chem. React. Eng.* **2014**, *12*, 397–403. [CrossRef]
11. Buglie, W.L.N.; Tamrin, K.F.; Sheikh, N.A.; Yasin, M.F.M.; Mohamaddan, S. Enhanced Fluid Mixing Using a Reversed Multistage Tesla Micromixer. *Chem. Eng. Technol.* **2022**, *45*, 1255–1263. [CrossRef]
12. Qian, J.Y.; Hou, C.W.; Li, X.J.; Jin, Z.J. Actuation Mechanism of Microvalves: A Review. *Micromachines* **2020**, *11*, 172. [CrossRef]
13. Nguyen, Q.M.; Huang, D.; Zauderer, E.; Romanelli, G.; Meyer, C.L.; Ristroph, L. Tesla's Fluidic Diode and the Electronic-Hydraulic Analogy. *Am. J. Phys.* **2021**, *89*, 393–402. [CrossRef]
14. Qian, J.-Y.; Wu, J.-Y.; Gao, Z.-X.; Wu, A.; Jin, Z.-J. Hydrogen Decompression Analysis by Multi-Stage Tesla Valves for Hydrogen Fuel Cell. *Int. J. Hydrog. Energy* **2019**, *44*, 13666–13674. [CrossRef]
15. Jin, Z.-J.; Gao, Z.-X.; Chen, M.-R.; Qian, J.-Y. Parametric Study on Tesla Valve with Reverse Flow for Hydrogen Decompression. *Int. J. Hydrog. Energy* **2018**, *43*, 8888–8896. [CrossRef]
16. Nobakht, A.Y.; Shahsavan, M.; Paykani, A. Numerical Study of Diodicity Mechanism in Different Tesla-Type Microvalves. *J. Appl. Res. Technol.* **2013**, *11*, 876–885. [CrossRef]
17. Tesař, V. Time-Delay Circuits for Fluidic Oscillators and Pulse Shapers. *Energies* **2019**, *12*, 3071. [CrossRef]
18. Bohm, S.; Phi, H.B.; Moriyama, A.; Runge, E.; Strehle, S.; König, J.; Cierpka, C.; Dittrich, L. Highly Efficient Passive Tesla Valves for Microfluidic Applications. *Microsyst. Nanoeng.* **2022**, *8*, 97. [CrossRef]
19. Anshori, I.; Lukito, V.; Adhawiyah, R.; Putri, D.; Harimurti, S.; Rajab, T.L.E.; Pradana, A.; Akbar, M.; Syamsunarno, M.R.A.A.; Handayani, M.; et al. Versatile and Low-Cost Fabrication of Modular Lock-and-Key Microfluidics for Integrated Connector Mixer Using a Stereolithography 3D Printing. *Micromachines* **2022**, *13*, 1197. [CrossRef]
20. Prabowo, B.A.; Purwidyantri, A. Environmentally Friendly and Biodegradable Components for Biosensors. *IEEE Nanotechnol. Mag.* **2022**, *16*, 13–19. [CrossRef]
21. Liu, Z.; Shao, W.-Q.; Sun, Y.; Sun, B.-H. Scaling Law of the One-Direction Flow Characteristics of Symmetric Tesla Valve. *Eng. Appl. Comput. Fluid Mech.* **2022**, *16*, 441–452. [CrossRef]
22. Lin, S.; Zhao, L.; Guest, J.K.; Weihs, T.P.; Liu, Z. Topology Optimization of Fixed-Geometry Fluid Diodes. *J. Mech. Des. Trans. ASME* **2015**, *137*, 081402. [CrossRef]
23. Gamboa, A.R.; Morris, C.J.; Forster, F.K. Optimization of the Fixed-Geometry Valve for Increased Micropump Performance. In Proceedings of the ASME 2003 International Mechanical Engineering Congress and Exposition, Washington, DC, USA, 15–21 November 2003; Volume 259, pp. 525–534.
24. Lam, R.H.W.; Li, W.J. A Digitally Controllable Polymer-Based Microfluidic Mixing Module Array. *Micromachines* **2012**, *3*, 279–294. [CrossRef]
25. Thompson, S.M.; Jamal, T.; Paudel, B.J.; Walters, D.K. Transitional and Turbulent Flow Modeling in a Tesla Valve. In Proceedings of the ASME International Mechanical Engineering Congress and Exposition, San Diego, CA, USA, 15–21 November 2013; Volume 7B.

26. de Vries, S.F.; Florea, D.; Homburg, F.G.A.; Frijns, A.J.H. Design and Operation of a Tesla-Type Valve for Pulsating Heat Pipes. *Int. J. Heat Mass Transf.* **2017**, *105*, 1–11. [CrossRef]
27. Turowski, M.; Chen, Z.; Przekwas, A. Automated Generation of Compact Models for Fluidic Microsystems. *Analog. Integr. Circuits Signal. Process.* **2001**, *29*, 27–36. [CrossRef]
28. Fairley, J.D.; Thompson, S.M.; Anderson, D. Time-Frequency Analysis of Flat-Plate Oscillating Heat Pipes. *Int. J. Therm. Sci.* **2015**, *91*, 113–124. [CrossRef]
29. Qian, J.-Y.; Chen, M.-R.; Liu, X.-L.; Jin, Z.-J. A Numerical Investigation of the Flow of Nanofluids through a Micro Tesla Valve. *J. Zhejiang Univ. Sci. A* **2019**, *20*, 50–60. [CrossRef]
30. Wahidi, T.; Chandavar, R.A.; Yadav, A.K. Stability Enhancement of Supercritical CO2 Based Natural Circulation Loop Using a Modified Tesla Valve. *J. Supercrit. Fluids* **2020**, *166*, 105020. [CrossRef]
31. Yao, Y.; Zhou, Z.; Liu, H.; Li, T.; Gao, X. Valveless Piezoelectric Pump with Reverse Diversion Channel. *Electronics* **2021**, *10*, 1712. [CrossRef]
32. Yang, X.; Song, F.; Wu, Y.; Guo, S.; Xu, S.; Zhou, J.; Liu, H. Suppression of Pressure Feedback of the Rotating Detonation Combustor by a Tesla Inlet Configuration. *Appl. Therm. Eng.* **2022**, *216*, 119123. [CrossRef]
33. Hu, P.; Wang, P.; Liu, L.; Ruan, X.; Zhang, L.; Xu, Z. Numerical Investigation of Tesla Valves with a Variable Angle. *Phys. Fluids* **2022**, *34*, 033603. [CrossRef]
34. Wang, J.; Cui, B.; Liu, H.; Chen, X.; Li, Y.; Wang, R.; Lang, T.; Yang, H.; Li, L.; Pan, H.; et al. Tesla Valve-Based Flexible Microhybrid Chip with Unidirectional Flow Properties. *ACS Omega* **2022**, *7*, 31744–31755. [CrossRef]
35. García-Morales, N.G.; Morales-Cruzado, B.; Camacho-López, S.; Romero-Méndez, R.; Devia-Cruz, L.F.; Pérez-Gutiérrez, F.G. Numerical Modeling of a Micropump without Mobile Parts Actuated by Thermocavitation Bubbles. *Microsyst. Technol.* **2021**, *27*, 801–812. [CrossRef]
36. Lu, Y.; Wang, J.; Liu, F.; Liu, Y.; Wang, F.; Yang, N.; Lu, D.; Jia, Y. Performance Optimisation of Tesla Valve-Type Channel for Cooling Lithium-Ion Batteries. *Appl. Therm. Eng.* **2022**, *212*, 118583. [CrossRef]
37. Thompson, S.M.; Paudel, B.J.; Jamal, T.; Walters, D.K. Numerical Investigation of Multistaged Tesla Valves. *J. Fluids Eng.* **2014**, *136*, 081102. [CrossRef]
38. Thompson, S.M.; Walters, D.K.; Paudel, B.J.; Jamal, T. A Numerical Investigation of Multi-Staged Tesla Valves. In Proceedings of the ASME 2013 Fluids Engineering Division Summer Meeting, Incline Village, NV, USA, 7–11 July 2013; Volume 1A.
39. Mohammadzadeh, K.; Kolahdouz, E.M.; Shirani, E.; Shafii, M.B. Numerical Study on the Performance of Tesla Type Microvalve in a Valveless Micropump in the Range of Low Frequencies. *J. Micro-Bio Robot.* **2013**, *8*, 145–159. [CrossRef]
40. Habhab, M.-B.; Ismail, T.; Lo, J.F. A Laminar Flow-Based Microfluidic Tesla Pump via Lithography Enabled 3D Printing. *Sensors* **2016**, *16*, 1970. [CrossRef]
41. Gaymann, A.; Montomoli, F.; Pietropaoli, M. Design for Additive Manufacturing: Valves without Moving Parts. In Proceedings of the ASME Turbo Expo 2017: Turbomachinery Technical Conference and Exposition, Charlotte, NC, USA, 26–30 June 2017; Volume 2C-2017.
42. Porwal, P.R.; Thompson, S.M.; Walters, D.K.; Jamal, T. Heat Transfer and Fluid Flow Characteristics in Multistaged Tesla Valves. *Numeri Heat Transf. A Appl.* **2018**, *73*, 347–365. [CrossRef]
43. Juodenas, M.; Tamulevičius, T.; Ulčinas, O.; Tamulevičius, S. Implementation of an Optimized Microfluidic Mixer in Alumina Employing Femtosecond Laser Ablation. *J. Micromech. Microeng.* **2018**, *28*, 015013. [CrossRef]
44. Qian, J.-Y.; Chen, M.-R.; Gao, Z.-X.; Jin, Z.-J. Mach Number and Energy Loss Analysis inside Multi-Stage Tesla Valves for Hydrogen Decompression. *Energy* **2019**, *179*, 647–654. [CrossRef]
45. Abdelwahed, M.; Chorfi, N.; Malek, R. Reconstruction of Tesla Micro-Valve Using Topological Sensitivity Analysis. *Adv. Nonlinear Anal.* **2019**, *9*, 567–590. [CrossRef]
46. Wen, Y.; Chen, R.-F. Study on Seepage Characteristics of Large Scale Tesla Valve and Feasibility of Its Application in Water Pipeline. *Shuidonglixue Yanjiu Yu Jinzhan/Chin. J. Hydrodyn Ser. A* **2020**, *35*, 726–735. [CrossRef]
47. Raffel, J.; Ansari, S.; Nobes, D.S. An Experimental Investigation of Flow Phenomena in a Multistage Micro-Tesla Valve. *J. Fluids Eng. Trans. ASME* **2021**, *143*, 111205. [CrossRef]
48. Shaikh, M.; Liu, X.; Amini, K.; Steinle, T.; Biegert, J. High Density Molecular Jets of Complex Neutral Organic Molecules with Tesla Valves. *Rev. Sci. Instrum.* **2021**, *92*, 104103. [CrossRef] [PubMed]
49. Monika, K.; Chakraborty, C.; Roy, S.; Sujith, R.; Datta, S.P. A Numerical Analysis on Multi-Stage Tesla Valve Based Cold Plate for Cooling of Pouch Type Li-Ion Batteries. *Int. J. Heat Mass Transf.* **2021**, *177*, 121560. [CrossRef]
50. Michalska, M.; Surmiak, M.A.; Maasoumi, F.; Senevirathna, D.C.; Chantler, P.; Li, H.; Li, B.; Zhang, T.; Lin, X.; Deng, H.; et al. Microfluidic Processing of Ligand-Engineered NiO Nanoparticles for Low-Temperature Hole-Transporting Layers in Perovskite Solar Cells. *Sol. RRL* **2021**, *5*, 2100342. [CrossRef]
51. Shi, H.; Cao, Y.; Zeng, Y.; Zhou, Y.; Wen, W.; Zhang, C.; Zhao, Y.; Chen, Z. Wearable Tesla Valve-Based Sweat Collection Device for Sweat Colorimetric Analysis. *Talanta* **2022**, *240*, 123208. [CrossRef] [PubMed]
52. Babaoğlu, N.U.; Parvaz, F.; Foroozesh, J.; Hosseini, S.H.; Ahmadi, G.; Elsayed, K. Analysis and Optimization of Multistage Tesla Valves by Computational Fluid Dynamics and a Multi-Objective Genetic Algorithm. *Chem. Eng. Technol.* **2022**, *45*, 2245–2253. [CrossRef]

53. Du, J.; Liu, Y.; Ren, F.; Guo, J.; Li, M.; Arman, S. Numerical Thermal Analysis of Cold Plate Embedded in Novel Multistage Tesla Valve. In Proceedings of the 2022 International Conference on Smart Manufacturing and Material Processing (SMMP2022), Shanghai, China, 12–13 August 2022; IOS Press: Amsterdam, The Netherlands, 2022; Volume 29, pp. 151–161.
54. Li, X.; Worrall, K.; Vedanthu, A.; Scott-George, A.; Harkness, P. The Pulse-Elevator: A Pump for Granular Materials. *Acta Astronaut.* **2022**, *200*, 33–41. [CrossRef]
55. Guo, K.; Chen, Y.; Zhou, Z.; Zhu, S.; Ni, Z.; Xiang, N. A Novel 3D Tesla Valve Micromixer for Efficient Mixing and Chitosan Nanoparticle Production. *Electrophoresis* **2022**, *43*, 2184–2194. [CrossRef]
56. Sun, L.; Li, J.; Xu, H.; Ma, J.; Peng, H. Numerical Study on Heat Transfer and Flow Characteristics of Novel Microchannel Heat Sinks. *Int. J. Therm. Sci.* **2022**, *176*, 107535. [CrossRef]
57. Rui, Z.; Zhao, F.; Sun, H.; Sun, L.; Peng, H. Experimental Research on Flow Boiling Thermal-Hydraulic Characteristics in Novel Microchannels. *Exp. Therm. Fluid Sci.* **2023**, *140*, 110755. [CrossRef]
58. Thompson, S.M.; Ma, H.B.; Wilson, C. Investigation of a Flat-Plate Oscillating Heat Pipe with Tesla-Type Check Valves. *Exp. Therm. Fluid Sci.* **2011**, *35*, 1265–1273. [CrossRef]
59. Sato, Y.; Yaji, K.; Izui, K.; Yamada, T.; Nishiwaki, S. Topology Optimization of a No-Moving-Part Valve Incorporating Pareto Frontier Exploration. *Struct. Multidiscip. Optim.* **2017**, *56*, 839–851. [CrossRef]
60. Guo, Y.; Pan, H.; Wadbro, E.; Liu, Z. Design Applicable 3D Microfluidic Functional Units Using 2D Topology Optimization with Length Scale Constraints. *Micromachines* **2020**, *11*, 613. [CrossRef]
61. Kubar, A.A.; Cheng, J.; Kumar, S.; Liu, S.; Chen, S.; Tian, J. Strengthening Mass Transfer with the Tesla-Valve Baffles to Increase the Biomass Yield of Arthrospira Platensis in a Column Photobioreactor. *Bioresour. Technol.* **2020**, *320*, 124337. [CrossRef]
62. Shalabi, N.; Searles, K.; Takahata, K. Switch Mode Capacitive Pressure Sensors. *Microsyst. Nanoeng.* **2022**, *8*, 1–14. [CrossRef]
63. Liosis, C.; Sofiadis, G.; Karvelas, E.; Karakasidis, T.; Sarris, I. A Tesla Valve as a Micromixer for Fe3O4 Nanoparticles. *Processes* **2022**, *10*, 1648. [CrossRef]
64. Wang, H.; Chen, X. Optimization of Micromixer Based on an Improved Tesla Valve-Typed Structure. *J. Braz. Soc. Mech. Sci. Eng.* **2022**, *44*, 1–11. [CrossRef]
65. Wang, H.; Chen, X. Optimization of Tesla Valve-Typed Micromixer Based on Simulated Annealing Algorithm. *Surf. Rev. Lett.* **2022**, *29*, 2250094. [CrossRef]
66. Wahidi, T.; Yadav, A.K. Instability Mitigation by Integrating Twin Tesla Type Valves in Supercritical Carbon Dioxide Based Natural Circulation Loop. *Appl. Therm. Eng.* **2021**, *182*, 116087. [CrossRef]
67. Fan, Y.; Wang, Z.; Xiong, X.; Zhu, J.; Gao, Q.; Wang, H.; Wu, H. Novel Concept Design of Low Energy Hybrid Battery Thermal Management System Using PCM and Multistage Tesla Valve Liquid Cooling. *Appl. Therm. Eng.* **2023**, *220*, 119680. [CrossRef]
68. Rajale, M.J.; Prasad, P.I.; Rao, B.N. A Review on the Heat Transfer Performance of Pulsating Heat Pipes. *Aust. J. Mech. Eng.* **2022**, 1–45. [CrossRef]
69. Prabowo, B.A.; Fernandes, E.; Freitas, P. A Pump-Free Microfluidic Device for Fast Magnetic Labeling of Ischemic Stroke Biomarkers. *Anal. Bioanal. Chem.* **2022**, *414*, 2571–2583. [CrossRef] [PubMed]
70. Gong, F.; Yang, X.; Zhang, X.; Mao, Z.; Gao, W.; Wang, C. The Study of Tesla Valve Flow Field on the Net Power of Proton Exchange Membrane Fuel Cell. *Appl. Energy* **2023**, *329*, 120276. [CrossRef]
71. Prabowo, B.A.; Sousa, C.; Cardoso, S.; Freitas, P.; Fernandes, E. Labeling on a Chip of Cellular Fibronectin and Matrix Metallopeptidase-9 in Human Serum. *Micromachines* **2022**, *13*, 1722. [CrossRef]
72. Leung, C.M.; de Haan, P.; Ronaldson-Bouchard, K.; Kim, G.A.; Ko, J.; Rho, H.S.; Chen, Z.; Habibovic, P.; Jeon, N.L.; Takayama, S.; et al. A Guide to the Organ-on-a-Chip. *Nat. Rev. Methods Prim.* **2022**, *2*, 33. [CrossRef]
73. Rogal, J.; Schlünder, K.; Loskill, P. Developer's Guide to an Organ-on-Chip Model. *ACS Biomater. Sci. Eng.* **2022**, *8*, 4643–4647. [CrossRef]
74. Moradi, E.; Jalili-Firoozinezhad, S.; Solati-Hashjin, M. Microfluidic Organ-on-a-Chip Models of Human Liver Tissue. *Acta Biomater.* **2020**, *116*, 67–83. [CrossRef]
75. Kanabekova, P.; Kadyrova, A.; Kulsharova, G. Microfluidic Organ-on-a-Chip Devices for Liver Disease Modeling In Vitro. *Micromachines* **2022**, *13*, 428. [CrossRef]
76. Gonçalves, I.M.; Carvalho, V.; Rodrigues, R.O.; Pinho, D.; Teixeira, S.F.C.F.; Moita, A.; Hori, T.; Kaji, H.; Lima, R.; Minas, G. Organ-on-a-Chip Platforms for Drug Screening and Delivery in Tumor Cells: A Systematic Review. *Cancers* **2022**, *14*, 935. [CrossRef]
77. Chen, Q.; Liu, X.; Lei, Y.; Zhu, H. An Electrokinetic Preconcentration Trapping Pattern in Electromembrane Microfluidics. *Phys. Fluids* **2022**, *34*, 092009. [CrossRef]
78. Wang, R.; Wang, X. Sensing of Inorganic Ions in Microfluidic Devices. *Sens. Actuators B Chem.* **2021**, *329*, 129171. [CrossRef]
79. Sabbagh, B.; Stolovicki, E.; Park, S.; Weitz, D.A.; Yossifon, G. Tunable Nanochannels Connected in Series for Dynamic Control of Multiple Concentration-Polarization Layers and Preconcentrated Molecule Plugs. *Nano Lett.* **2020**, *20*, 8524–8533. [CrossRef]
80. Krishnamurthy, A.; Anand, R.K. Recent Advances in Microscale Extraction Driven by Ion Concentration Polarization. *Trends Anal. Chem.* **2022**, *148*, 116537. [CrossRef]
81. Papadimitriou, V.A.; Segerink, L.I.; Eijkel, J.C.T. Free Flow Ion Concentration Polarization Focusing (FF-ICPF). *Anal. Chem.* **2020**, *92*, 4866–4874. [CrossRef]

82. Andriukaitis, D.; Vargalis, R.; Šerpytis, L.; Drevinskas, T.; Kornyšova, O.; Stankevičius, M.; Bimbiraitė-Survilienė, K.; Kaškonienė, V.; Maruškas, A.S.; Jonušauskas, L. Fabrication of Microfluidic Tesla Valve Employing Femtosecond Bursts. *Micromachines* **2022**, *13*, 1180. [CrossRef]
83. Bachman, H.; Chen, C.; Rufo, J.; Zhao, S.; Yang, S.; Tian, Z.; Nama, N.; Huang, P.H.; Huang, T.J. An Acoustofluidic Device for Efficient Mixing over a Wide Range of Flow Rates. *Lab Chip* **2020**, *20*, 1238–1248. [CrossRef]
84. Huang, P.H.; Nama, N.; Mao, Z.; Li, P.; Rufo, J.; Chen, Y.; Xie, Y.; Wei, C.H.; Wang, L.; Huang, T.J. A Reliable and Programmable Acoustofluidic Pump Powered by Oscillating Sharp-Edge Structures. *Lab Chip* **2014**, *14*, 4319–4323. [CrossRef]
85. Lee, S.W.; Kim, D.S.; Lee, S.S.; Kwon, T.H. A Split and Recombination Micromixer Fabricated in a PDMS Three-Dimensional Structure. *J. Micromech. Microeng.* **2006**, *16*, 1067–1072. [CrossRef]